

# UCSF

## UC San Francisco Previously Published Works

### Title

Neuroimaging of Peptide-based Vaccine Therapy in Pediatric Brain Tumors Initial Experience

### Permalink

<https://escholarship.org/uc/item/9568d2s3>

### Journal

Neuroimaging Clinics of North America, 27(1)

### ISSN

1052-5149

### Authors

Furtado, Andre D  
Ceschin, Rafael  
Blüml, Stefan  
[et al.](#)

### Publication Date

2017-02-01

### DOI

10.1016/j.nic.2016.09.002

Peer reviewed



# HHS Public Access

Author manuscript

*Neuroimaging Clin N Am.* Author manuscript; available in PMC 2018 February 01.

Published in final edited form as:

*Neuroimaging Clin N Am.* 2017 February ; 27(1): 155–166. doi:10.1016/j.nic.2016.09.002.

## Neuroimaging of Peptide Based Vaccine Therapy in Pediatric Brain Tumors: Initial Experience

Andre D. Furtado, M.D.<sup>1</sup>, Rafael Ceschin, B.S.<sup>1,2</sup>, Stefan Bluml, Ph.D.<sup>6</sup>, Jack Schnur<sup>1</sup>, Gary Mason, M.D.<sup>3</sup>, Regina I. Jakacki, M.D.<sup>3</sup>, Hideho Okada, M.D.<sup>7</sup>, Ian F. Pollack, M.D.<sup>4,5</sup>, and Ashok Panigrahy, MD<sup>1,2,5</sup>

<sup>1</sup>Department of Radiology, University of Pittsburgh, Pittsburgh, PA, USA

<sup>2</sup>Department of Bioinformatics, University of Pittsburgh, Pittsburgh, PA, USA

<sup>3</sup>Department of Pediatrics, University of Pittsburgh, Pittsburgh, PA, USA

<sup>4</sup>Department of Neurosurgery, University of Pittsburgh, Pittsburgh, PA, USA

<sup>5</sup>University of Pittsburgh School of Medicine, Children's Hospital of Pittsburgh, University of Pittsburgh Cancer Institute, University of Pittsburgh, Pittsburgh, PA, USA

<sup>6</sup>Department of Radiology, University of California, San Francisco, CA

<sup>7</sup>Childrens Hospital of Los Angeles and Department of Neurosurgery, University of California, San Francisco, CA

### Abstract

The potential benefits of peptide-based immunotherapy for pediatric brain tumors is currently under investigation with pilot studies at our institution. We have noted the presence of treatment-related heterogeneity, which has resulted in radiographic challenges including that of pseudoprogression. Conventional MRI has limitations in the assessment of these different forms of treatment-related heterogeneity, particularly in regards to distinguishing true tumor progression from efficacious treatment responses. Our initial results suggest that advanced neuroimaging techniques, including diffusion MR, perfusion MR and MR spectroscopy may add value in the assessment of treatment-related heterogeneity. Our initial observations suggests that recent delineation of specific response criteria for immunotherapy of adult brain tumors (iRANO) is likely to be relevant to the pediatric population and further validation in multi-center pediatric brain tumor peptide-based vaccine studies are warranted.

---

Address Correspondence and Reprint Request to: Ashok Panigrahy, MD, Department of Pediatric Radiology, Children's Hospital of Pittsburgh of UPMC, 4401 Penn Avenue, Pittsburgh, PA 15224, Tel: 412-692-5510, Fax: 412-864-8622, panigrahya@upmc.edu.

**Conflicts of Interest:** Hideho Okada is an inventor in the U.S. Patent Application No. 60,611, 797 (Utility Patent Application) "Identification of An IL-13 Receptor Alpha2 Peptide Analogue Capable of Enhancing Stimulation of Glioma-Specific CTL Response". An exclusive licensing agreement has been completed on this application between University of Pittsburgh and Stemline, Inc. Due to the potential conflicts of interest, Hideho Okada did not solely interpret any data in the current study. Dr. Regina I. Jakacki is currently employed by Astra Zeneca.

**Publisher's Disclaimer:** This is a PDF file of an unedited manuscript that has been accepted for publication. As a service to our customers we are providing this early version of the manuscript. The manuscript will undergo copyediting, typesetting, and review of the resulting proof before it is published in its final citable form. Please note that during the production process errors may be discovered which could affect the content, and all legal disclaimers that apply to the journal pertain.

## Keywords

pseudoprogression; vaccine therapy; pediatric brain tumors; MR spectroscopy

---

## Introduction

There has been significant progress in the field of immunotherapy, within oncology with recent FDA approval of immunotherapeutics for metastatic melanoma and non-small cell lung cancer, and the advent of multiple immunotherapy clinical trials for primary and metastatic adult brain tumors. [1-4] These adult immunotherapy studies have identified unique responses in regards to treatment response heterogeneity (as characterized by pseudoprogression, delayed responses, therapy-induced inflammation, etc.) and resulting radiographic challenges. As such, new guidelines have been recently published by the iRANO (immunotherapy Response Assessment for Neuro-Oncology) group to allow for refinement of response assessment criteria for neurooncology patients receiving immunotherapy. [4] These iRANO criteria suggest that among adult patients who demonstrate imaging findings meeting RANO criteria for progressive disease within 6 months of initiating immunotherapy, including the development of new lesions, confirmation of radiographic progression on follow-up imaging is recommended provided that the adult patient is not significantly worse clinically.[4]

Our institution is currently engaged in multiple peptide based- vaccine trials for children with diffuse midline gliomas (DIPG), recurrent high-grade glioma, recurrent low grade-glioma and recurrent ependymoma [5-7], We have recently described the occurrence of heterogeneous treatment response (including pseudoprogression) which has remarkable similarity with what has been seen in some of the adult immunotherapy studies. The purpose of this review article is to highlight our initial experience with regards to the emerging radiographic challenges related to heterogeneous treatment response including that of pseudoprogression with the use of peptide-based vaccine therapy in pediatric brain tumors. We also describe our initial experience with some of the advanced neuroimaging techniques including diffusion MR and MR spectroscopy to help address some of these radiographic challenges.

## Conventional MRI

We have noted multiple forms of treatment-related heterogeneity in our different pilot studies of peptide-based vaccine therapy for pediatric brain tumors, particularly in DIPG, recurrent supra-tentorial high-grade tumors, and recurrent low grade-gliomas. Conventional MR imaging supplemented with MRS, diffusion and perfusion MR was typically performed serially at regular intervals depending on the specific protocol while on the peptide-based vaccine therapy (Figure 1) (i.e. every 6 weeks for newly diagnosed patients who are receiving radiation). The different forms of treatment-related heterogeneity that have resulted in radiographic challenges include (1) pseudoprogression, characterized by transient enlargement of the tumor with associated clinical symptoms, recently published for our DIPG cohort (Figure 2A) and recurrent low grade glioma cohort [5, 6]; (2) development of different types of non-cystic and cystic focal signal abnormalities within our DIPG and

recurrent supratentorial high-grade glioma cohort (see next paragraph and Figure 3); (3) development of both contiguous (Figure 2B) and remote smaller lesion that eventually regress and/or undergo necrosis; (4) one portion of the tumor responds to treatment while another portion of the tumor appears to be growing (Figure 7).

In a series of 21 children with diffuse intrinsic pontine glioma (DIPG) treated with peptide-based vaccines at our institution, 4 children (19%) had documented pseudoprogression based on imaging and clinical criteria: one child had transient tumor enlargement in association with acute neurological deterioration 4 months after beginning vaccination that later regressed and culminated in a sustained partial response (Figure 2A); and 3 other children had symptomatic pseudoprogression, with transient neurological deterioration and tumor enlargement followed by stabilization on decreasing steroid doses. Notably, after the episode of pseudoprogression, the patient with the subsequent PR developed contiguous lesions in the bilateral middle cerebellar peduncle later in the course of peptide-based vaccine therapy. These lesions eventually underwent shrinkage and necrosis (Fig 2B). Cases of pseudoprogression were also noted in other types of pediatric brain tumors being treated with the peptide vaccine including a cervicomedullary biopsy proven anaplastic astrocytoma lesion (Figure 3), recurrent supratentorial high grade and recurrent low-grade gliomas [5, 6].

We also observed an unusually high incidence of focal cystic and non-cystic signal intensity changes (likely representing evolving necrosis) in our pediatric DIPG population treated with the peptide-based vaccine. When we classified these changes into four categories based on T2 signal characteristics and post-contrast enhancement characteristics (Figure 4), we found that 81% of these children developed focal areas of non-cystic changes during immunotherapy with an average time between starting vaccine to development of non cystic changes of 4.8 months (from 38 days to 10.8 months) and 57% developed focal cystic changes with an average time of 6.5 months (from 1.2 months to 10.6 months) after the initiation of therapy. Of all the patients who developed cystic necrosis, 82% had noticeable enhancement in the region prior to the development of the necrosis. A small subset of patients had areas of enhancement that were stable or decrease in size on subsequent exams. Studies are on-going at our institution to correlate these patterns of focal signal abnormality with survival and pseudoprogression. These findings do underscore the concept that conventional MRI imaging has limitations in the ability to assess different forms of treatment related imaging heterogeneity. In the next sections, we describe our initial experience with the use of advanced neuroimaging modalities (i.e. MR spectroscopy, diffusion and perfusion) to evaluate treatment response.

### **Magnetic Resonance Spectroscopy**

Magnetic resonance spectroscopy provides a metabolic evaluation of the sampled tissue. In vivo Intracellular metabolites with concentrations of 0.1-0.5  $\mu\text{mol}/\text{gram}$  or higher can be assessed. Abnormal choline (Cho) metabolism is a common endpoint for many forms of cancer. Choline containing metabolites are involved in the synthesis and breakdown of cell membranes. Since growing tumors require the net synthesis of cell membranes to support cell proliferation, the in vivo measurement of choline provides surrogate information on tumor growth rates. Brain tumors generally have elevated levels of Cho, with higher Cho

levels observed in more aggressive tumors [8-10]. Another metabolic feature of aggressive tumors is a prominent signal from mobile lipids [11, 12], although the time course is less predictable. Lipids (and lactate) can accumulate in cystic/necrotic areas but may also be recycled by tumor cells and/or surrounding cells for de novo cell membrane synthesis and for oxidation in the TCA-cycle. Lipids may increase as tumors progress, for example, from grade III astrocytoma to glioblastoma [12]. Notably, myo-inositol is well-regarded as a marker of gliosis [13] as well as an important osmolyte whose regulation across the plasma membrane is a key cellular mechanism for mediating osmotic stress in astrocytes [14, 15]. In-vivo human studies, myo-inositol is consistently elevated in the setting of chronic inflammation such as in multiple sclerosis and other neuroinflammatory CNS conditions [16-18] likely reflecting ongoing astrogliosis. Myo-inositol is generally elevated in ependymoma and gliomas, which are typically characterized by a high fraction of glial cells [19-21]. Histopathological studies have suggested there is increased reactive gliosis in individual tumors marked by an elevated myo-inositol concentration [22, 23], and in a recent study, elevated myo-inositol distinguished tissue inflammation from tumor proliferation in adult GBM patients treated with radiation therapy and adjuvant therapy [24]. We are currently exploring the hypothesis that alterations in myo-inositol may be a predictor of outcome in certain forms of pediatric tumors treated with the peptide base vaccines (particularly the DIPG cohort- Figure 5). A key observation was the stability of serial MRS spectra in the setting of clinical and radiographic pseudoprogession (Figure 5). Specifically, we noted that the MRS spectra was stable comparing three time points of imaging: baseline, at the time of pseudoprogession and after pseudoprogession. When we looked specifically at the cases of pseudoprogession (i.e. case shown in Figure 2), there was serial stability in the choline to creatine ratio, myo-inositol and lipids/lactate (bottom row, Figure 5). From these preliminary observations, we hypothesize that the stability of certain metabolite ratios (including choline/creatine ratio) may distinguish treatment response and pseudoprogession from true progession in the setting of peptide-based treatment of high-grade gliomas (including DIPG). Likewise, stability in lipids/lactate and myo-inositol may also have the potential to distinguish pseudoprogession from true progession. These findings underscore the importance in obtaining serial MRS data at baseline and different points of therapy, including at the time of pseudoprogession. These preliminary observations will need to be confirmed in large-scale multi-center studies.

### Diffusion Weighted MR Imaging

Diffusion refers to random (“Brownian”) motion of molecules due to heat. In clinical imaging, we evaluate the mean diffusivity of water molecules assuming isotropy in each voxel. In vivo, the limitation of diffusion-weighted imaging (DWI) is that the diffusion of water molecules is not only due to heat, but also active transport, flow along pressure gradients, and changes in membrane permeability. The apparent diffusion coefficient (ADC) is a quantitative diffusion constant calculated from different b values (different gradient amplitudes) to reflect the diffusion of water molecules through different tissues, expressed in units of  $\text{mm}^2/\text{s}$  [25]. Higher ADC values mean increased water motion and lower ADC values mean decreased (restricted) water motion. Although untreated brain tumors demonstrate increased ADC values compared to the normal brain as a result of disruption of normal cellular integrity, densely cellular tumors demonstrate relative lower ADC values.

Baseline low minimum ADC values have been associated with worse clinical outcome as determined by us and others [26, 27]. The effect of radiation therapy can be divided in acute, early-delayed, and late-delayed radiation changes. A transient increase in ADC has been reported between 3 and 5 months after radiation [28], likely the result from tissue damage, vasodilation and edema [29]. With time the ADC values decrease, which is particularly noticeable in children with DIPG (Figure 6, left). Using serial functional diffusion maps (sfDM), our group demonstrated that children with DIPG status post radiation, who had tumor pseudoprogression during immunotherapy had higher fitted average log-transformed parametric response mapping ratios and fractional decreased ADC, compared to those without pseudoprogression [30]. Moreover, focal increase in ADC signal preceded the appearance of cystic necrosis (Figure 6, right). Serial parametric response mapping of ADC appears to be a promising method to assess treatment response in children with DIPG treated with peptide-based vaccinations.

### Perfusion MR Imaging

The three major types of perfusion MR that we performed in our studies of pediatric brain tumors treated with peptide-based vaccine therapy include: Dynamic Susceptibility Contrast, Dynamic Contrast Enhancement and Arterial Spin Labeling. Dynamic susceptibility contrast (DSC) MRI, also known as bolus-tracking MRI, is based on serial measurements of MRI signal change within a region of interest during the first pass of exogenous, paramagnetic, non diffusible contrast agent, typically a gadolinium-based contrast agent (GBCA). Under normal conditions, the local susceptibility effect induced by intravascular compartmentalization of GBCA translates into a signal drop on T2 spin-echo or gradient-echo (T2\* GRE) echo planar imaging (EPI). Higher-grade brain tumors tend to have increased microvascular circulation related to tumoral angiogenesis and, as a result, larger blood volume on DSC signal intensity time curves [31]. This technique is very valuable for guidance of stereotactic biopsy. One of the limitations of DSC is when there is severe disruption of the brain-blood barrier causing inaccurate estimation of intravascular blood volume due to extravasation of GBCA (T1 dominant contrast leakage) [32, 33]. In contrast to DSC imaging, dynamic contrast enhanced (DCE) imaging measures an increase in MRI signal proportional to the concentration of GBCA in the region of interest using T1-weighted imaging, providing an evaluation of the wash-in and washout contrast kinetics within tumors as a result of tumor perfusion, vessel permeability, and volume of the extravascular-extracellular space [34]. One alternative without the administration of intravenous contrast is the arterial spin labeling (ASL), which consists of labeling protons in the blood in supplying vessels outside the imaging plane. Subtraction of the images obtained with and without labeling allows calculation of tissue perfusion, which is proportional to the cerebral blood flow (CBF) [35]. ASL may be a reliable alternative to DSC with several advantages in children because of it does not require intravenous administration of contrast, can be repeated multiple times, and has the potential to provide quantitative CBF [36]. In a recent article by the Pediatric Brain Tumor Consortium, there was no association between progression free survival and relative cerebral blood volume assess by DSC at baseline, or when perfusion values were used as time-dependent variables, in children with brain tumor treated with radiation and molecularly targeted agents (gefitinib and tipifarnib) [27].

The potential role of DSC, DCE and ASL imaging in assessing pediatric brain tumor treated with immunotherapy is currently being investigated at our institution. As a pilot study, we have examined diffusion and perfusion correlates of heterogeneous treatment response in peptide-based therapy of pediatric DIPG. We tested the hypothesis that correlations between ADC (cellularity) and ASL (vascularity) would differ between brainstem glioma (DIPG) groups treated with and without vaccine therapy. ADC and ASL images of 19 pediatric DIPG patients (n=11 on vaccine therapy, n=8 not on vaccine therapy) were acquired at 1.5T. After registration, tumor regions were manually segmented. A correlation analysis between mean ADC and ASL in the tumor and unaffected grey matter was conducted using linear regression. Statistically significant correlation between mean ADC and ASL were seen in DIPG regions of patients on vaccine (R=-0.358, p=0.0256). However, no statistically significant association was seen in the mean ADC and ASL of the DIPG in patients treated with standard radiation and radiochemotherapy (non-vaccine) (R=0.006, p=0.9770). As such, a unique inverse correlation of perfusion and diffusion (with increased perfusion associated with decreased ADC or increased cellularity) was noted in the vaccine therapy DIPG group compared to the non-vaccine therapy group. This may reflect identification of a unique treatment response within the vaccine group. Validation in a larger dataset and correlation with outcome is currently being pursued.

### **<sup>23</sup>Na-MR and [18F]-FLT Imaging**

<sup>23</sup>Na-MR is a useful non-invasive technique to assess proliferation. In neoplastic tissue, sustained depolarization of the cell membrane precedes the high rate of mitotic activity that characterizes abnormal tumor growth, leading to concomitant increase in intracellular <sup>23</sup>Na concentration (ISC) as demonstrated in a number of human neoplasms. Further characterization of this rise in ISC in several types of human carcinoma/glioma cell lines has established a positive correlation between proliferative activity and increased intracellular Na<sup>+</sup>/K<sup>+</sup> ratio. The increase in ISC leads to a concomitant increase in the total tissue <sup>23</sup>Na concentration (TSC) over the tumor volume [37-43]. <sup>23</sup>Na concentration was altered in a number of our pediatric patients with brain tumors treated with immunotherapy. The highest concentrations were observed in high-grade supratentorial astrocytomas (Figure 7). We have preliminarily observed that a decrease in <sup>23</sup>Na signal portends a good treatment response, possibly earlier than other imaging methods. We are currently evaluating the utility of sodium MR imaging to help characterize heterogeneous treatment response in different types of pediatric brain tumors undergoing peptide based vaccine therapy.

All of the MR biomarkers being studied (conventional MRI, MRS, ADC, ASL and sodium) have limitations in the assessment of new large necrotic lesions, which have been observed in a significant percentage of malignant gliomas treated with immunotherapy in our current clinical trials. 3'-[18F] fluoro-3'-deoxythymidine ([18F]-FLT) positron emission tomography may be particularly valuable for these patients. [18F]-FLT is a pyrimidine analogue and a biomarker for thymidine kinase-1 activity during S phase of DNA synthesis. Previous investigations have demonstrated a high correlation between [18F]-FLT uptake and proliferation rate [44-56]. The potential advantages of [18F]-FLT over [18F]-FDG in high-grade gliomas include: improved signal to noise ratio and significantly greater specificity for proliferation over treatment-related necrosis [57, 58]. In addition, there is research to support



that [18F]-FLT may distinguish between tumor proliferation and inflammation, which may be useful in the assessment of pseudoprogression [59-62]. We use [18F]-FLT to label solid tumor around areas of necrosis thereby potentially providing an indicator of tumor proliferation. We are currently in the process of developing a MR-PET protocol to perform [18F]-FLT imaging in our pediatric brain tumor patients being treated with peptide-based vaccine therapy.

## Conclusion

Potential benefits of peptide-based immunotherapy for pediatric brain tumors have been identified with pilot studies performed at our institution. We have described different forms of treatment-related heterogeneity, which has resulted in radiographic challenges including the determination of pseudoprogression vs. true tumor progression by conventional MRI. Our initial results suggest that advanced neuroimaging techniques, including diffusion MR, perfusion MR and MR spectroscopy may add value to the assessment of treatment-related heterogeneity. Future work may help identify which imaging approach is superior. Our initial observations suggest that recent delineation of specific response criteria for immunotherapy of adult brain tumors (iRANO) is likely to be relevant to the pediatric brain tumor population and further validation in multi-center pediatric brain tumor peptide-based vaccine studies are warranted.

## Acknowledgments

UPCI Clinical Research Services for regulatory management, Andres Salazar, Oncovir, Inc., for provision of poly-ICLC, physicians who referred their patients, and the patients and families who participated in this trial. This study was supported by National Institutes of Health grants R21CA149872, P01NS40923, and the UPCI Immunological Monitoring Core and Biostatistics Shared Resource Facility, supported in part by NIH award P30CA47904; grants from the Pediatric Low-Grade Glioma Initiative via the National Brain Tumor Society, the Ian's (Ian Yagoda) Friends Foundation Grant, Society of Pediatric Radiology Pilot Award and the Ellie Kavalieros Fund of the Children's Hospital of Pittsburgh Foundation; and the Pediatric Clinical and Translational Research Center, supported by the NIH through Grant Numbers UL1 RR024153 and UL1TR000005. We also thank Vince Lee with technical assistant and Fern Wasco with research coordination, RC was supported by a NLM Grant 5T15LM007059-27

## References

1. Kantoff PW, et al. Sipuleucel-T immunotherapy for castration-resistant prostate cancer. *N Engl J Med.* 2010; 363(5):411–22. [PubMed: 20818862]
2. Hodi FS, et al. Improved survival with ipilimumab in patients with metastatic melanoma. *N Engl J Med.* 2010; 363(8):711–23. [PubMed: 20525992]
3. Robert C, et al. Nivolumab in previously untreated melanoma without BRAF mutation. *N Engl J Med.* 2015; 372(4):320–30. [PubMed: 25399552]
4. Okada H, et al. Immunotherapy response assessment in neuro-oncology: a report of the RANO working group. *Lancet Oncology.* 2015; 16:534–42.
5. Pollack IF, et al. Immune responses and outcome after vaccination with glioma-associated antigen peptides and poly-ICLC in a pilot study for pediatric recurrent low-grade gliomas. *Neuro Oncol.* 2016
6. Pollack IF, et al. Antigen-specific immune responses and clinical outcome after vaccination with glioma-associated antigen peptides and polyinosinic-polycytidylic acid stabilized by lysine and carboxymethylcellulose in children with newly diagnosed malignant brainstem and nonbrainstem gliomas. *J Clin Oncol.* 2014; 32(19):2050–8. [PubMed: 24888813]



7. Yeung JT, et al. Increased expression of tumor-associated antigens in pediatric and adult ependymomas: implication for vaccine therapy. *J Neurooncol.* 2013; 111(2):103–11. [PubMed: 23179498]
8. Astrakas LG, et al. Noninvasive magnetic resonance spectroscopic imaging biomarkers to predict the clinical grade of pediatric brain tumors. *Clin Cancer Res.* 2004; 10(24):8220–8. [PubMed: 15623597]
9. Shimizu H, et al. Correlation between choline level measured by proton MR spectroscopy and Ki-67 labeling index in gliomas. *AJNR Am J Neuroradiol.* 2000; 21(4):659–65. [PubMed: 10782774]
10. Tamiya T, et al. Proton magnetic resonance spectroscopy reflects cellular proliferative activity in astrocytomas. *Neuroradiology.* 2000; 42(5):333–8. [PubMed: 10872152]
11. Negendank W, Sauter R. Intratumoral lipids in 1H MRS in vivo in brain tumors: experience of the Siemens cooperative clinical trial. *Anticancer Res.* 1996; 16(3b):1533–8. [PubMed: 8694522]
12. Murphy PS, et al. Could assessment of glioma methylene lipid resonance by in vivo (1)H-MRS be of clinical value? *Br J Radiol.* 2003; 76(907):459–63. [PubMed: 12857705]
13. Brand A, Richter-Landsberg C, Leibfritz D. Multinuclear NMR studies on the energy metabolism of glial and neuronal cells. *Dev Neurosci.* 1993; 15(3-5):289–98. [PubMed: 7805581]
14. Wiese TJ, et al. Osmotic regulation of Na-myoinositol cotransporter mRNA level and activity in endothelial and neural cells. *Am J Physiol.* 1996; 270(4 Pt 1):C990–7. [PubMed: 8928755]
15. Paredes A, et al. Osmoregulation of Na(+)-inositol cotransporter activity and mRNA levels in brain glial cells. *Am J Physiol.* 1992; 263(6 Pt 1):C1282–8. [PubMed: 1476169]
16. Kapeller P, et al. Discrimination of white matter lesions and multiple sclerosis plaques by short echo quantitative 1H-magnetic resonance spectroscopy. *J Neurol.* 2005; 252(10):1229–34. [PubMed: 15895306]
17. Bruhn H, et al. Multiple sclerosis in children: cerebral metabolic alterations monitored by localized proton magnetic resonance spectroscopy in vivo. *Ann Neurol.* 1992; 32(2):140–50. [PubMed: 1324631]
18. Chang L, et al. A multicenter in vivo proton-MRS study of HIV-associated dementia and its relationship to age. *Neuroimage.* 2004; 23(4):1336–47. [PubMed: 15589098]
19. Davies NP, et al. Identification and characterisation of childhood cerebellar tumours by in vivo proton MRS. *NMR Biomed.* 2008; 21(8):908–18. [PubMed: 18613254]
20. Panigrahy A, et al. Quantitative short echo time 1H-MR spectroscopy of untreated pediatric brain tumors: preoperative diagnosis and characterization. *AJNR Am J Neuroradiol.* 2006; 27(3):560–72. [PubMed: 16551993]
21. Panigrahy A, Bluml S. Neuroimaging of pediatric brain tumors: from basic to advanced magnetic resonance imaging (MRI). *J Child Neurol.* 2009; 24(11):1343–65. [PubMed: 19841424]
22. Hattingen E, et al. Myo-inositol: a marker of reactive astrogliosis in glial tumors? *NMR Biomed.* 2008; 21(3):233–41. [PubMed: 17562554]
23. Amstutz DR, et al. Hypothalamic hamartomas: Correlation of MR imaging and spectroscopic findings with tumor glial content. *AJNR Am J Neuroradiol.* 2006; 27(4):794–8. [PubMed: 16611766]
24. Srinivasan R, et al. Ex vivo MR spectroscopic measure differentiates tumor from treatment effects in GBM. *Neuro Oncol.* 2010; 12(11):1152–61. [PubMed: 20647244]
25. Mukherjee P, et al. Diffusion tensor MR imaging and fiber tractography: theoretic underpinnings. *AJNR Am J Neuroradiol.* 2008; 29(4):632–41. [PubMed: 18339720]
26. Okada H, et al. Autologous glioma cell vaccine admixed with interleukin-4 gene transfected fibroblasts in the treatment of patients with malignant gliomas. *J Transl Med.* 2007; 5:67. [PubMed: 18093335]
27. Poussaint TY, et al. MRI as a central component of clinical trials analysis in brainstem glioma: a report from the Pediatric Brain Tumor Consortium (PBTC). *Neuro Oncol.* 2011; 13(4):417–27. [PubMed: 21297126]
28. Kitahara S, et al. Evaluation of treatment-induced cerebral white matter injury by using diffusion-tensor MR imaging: initial experience. *AJNR Am J Neuroradiol.* 2005; 26(9):2200–6. [PubMed: 16219822]

29. Wong CS, Van der Kogel AJ. Mechanisms of radiation injury to the central nervous system: implications for neuroprotection. *Mol Interv.* 2004; 4(5):273–84. [PubMed: 15471910]
30. Ceschin R, et al. Parametric Response Mapping of Apparent Diffusion Coefficient as an Imaging Biomarker to Distinguish Pseudoprogression from True Tumor Progression in Peptide-Based Vaccine Therapy for Pediatric Diffuse Intrinsic Pontine Glioma. *AJNR Am J Neuroradiol.* 2015
31. Law M, et al. Comparison of cerebral blood volume and vascular permeability from dynamic susceptibility contrast-enhanced perfusion MR imaging with glioma grade. *AJNR Am J Neuroradiol.* 2004; 25(5):746–55. [PubMed: 15140713]
32. Cha S. Dynamic susceptibility-weighted contrast-enhanced perfusion MR imaging in pediatric patients. *Neuroimaging Clin N Am.* 2006; 16(1):137–47. ix. [PubMed: 16543089]
33. Calamante F. Perfusion MRI using dynamic-susceptibility contrast MRI: quantification issues in patient studies. *Top Magn Reson Imaging.* 2010; 21(2):75–85. [PubMed: 21613873]
34. Choyke PL, Dwyer AJ, Knopp MV. Functional tumor imaging with dynamic contrast-enhanced magnetic resonance imaging. *J Magn Reson Imaging.* 2003; 17(5):509–20. [PubMed: 12720260]
35. Pollock JM, et al. Arterial spin-labeled MR perfusion imaging: clinical applications. *Magn Reson Imaging Clin N Am.* 2009; 17(2):315–38. [PubMed: 19406361]
36. Yang Y, et al. Multislice imaging of quantitative cerebral perfusion with pulsed arterial spin labeling. *Magn Reson Med.* 1998; 39(5):825–32. [PubMed: 9581614]
37. Bartha R, Megyesi JF, Watling CJ. Low-grade glioma: correlation of short echo time 1H-MR spectroscopy with 23Na MR imaging. *AJNR Am J Neuroradiol.* 2008; 29(3):464–70. [PubMed: 18238848]
38. Cameron IL, et al. Intracellular concentration of sodium and other elements as related to mitogenesis and oncogenesis in vivo. *Cancer Res.* 1980; 40(5):1493–500. [PubMed: 7370987]
39. Ouwerkerk R, et al. Tissue sodium concentration in human brain tumors as measured with 23Na MR imaging. *Radiology.* 2003; 227(2):529–37. [PubMed: 12663825]
40. Thulborn KR, et al. Quantitative tissue sodium concentration mapping of the growth of focal cerebral tumors with sodium magnetic resonance imaging. *Magn Reson Med.* 1999; 41(2):351–9. [PubMed: 10080284]
41. Turski PA, et al. Experimental and human brain neoplasms: detection with in vivo sodium MR imaging. *Radiology.* 1987; 163(1):245–9. [PubMed: 3029803]
42. Boada FE, et al. Non-invasive assessment of tumor proliferation using triple quantum filtered 23Na MRI: technical challenges and solutions. *Conf Proc IEEE Eng Med Biol Soc.* 2004; 7:5238–41. [PubMed: 17271521]
43. Schepkin VD, et al. Proton and sodium MRI assessment of emerging tumor chemotherapeutic resistance. *NMR Biomed.* 2006; 19(8):1035–42. [PubMed: 16894643]
44. Chen W, et al. Imaging proliferation in brain tumors with 18F-FLT PET: comparison with 18F-FDG. *J Nucl Med.* 2005; 46(6):945–52. [PubMed: 15937304]
45. Shields AF, et al. Imaging proliferation in vivo with [F-18]FLT and positron emission tomography. *Nat Med.* 1998; 4(11):1334–6. [PubMed: 9809561]
46. Backes H, et al. Noninvasive quantification of 18F-FLT human brain PET for the assessment of tumour proliferation in patients with high-grade glioma. *Eur J Nucl Med Mol Imaging.* 2009; 36(12):1960–7. [PubMed: 19672593]
47. Hatakeyama T, et al. 11C-methionine (MET) and 18F-fluorothymidine (FLT) PET in patients with newly diagnosed glioma. *Eur J Nucl Med Mol Imaging.* 2008; 35(11):2009–17. [PubMed: 18542957]
48. Saga T, et al. Evaluation of primary brain tumors with FLT-PET: usefulness and limitations. *Clin Nucl Med.* 2006; 31(12):774–80. [PubMed: 17117071]
49. Ullrich R, et al. Glioma proliferation as assessed by 3'-fluoro-3'-deoxy-L-thymidine positron emission tomography in patients with newly diagnosed high-grade glioma. *Clin Cancer Res.* 2008; 14(7):2049–55. [PubMed: 18381944]
50. Chen W, et al. Predicting treatment response of malignant gliomas to bevacizumab and irinotecan by imaging proliferation with [18F] fluorothymidine positron emission tomography: a pilot study. *J Clin Oncol.* 2007; 25(30):4714–21. [PubMed: 17947718]

51. Choi SJ, et al. [18F]3'-deoxy-3'-fluorothymidine PET for the diagnosis and grading of brain tumors. *Eur J Nucl Med Mol Imaging*. 2005; 32(6):653–9. [PubMed: 15711980]
52. Yamamoto Y, et al. Correlation of 18F-FLT uptake with tumor grade and Ki-67 immunohistochemistry in patients with newly diagnosed and recurrent gliomas. *J Nucl Med*. 2012; 53(12):1911–5. [PubMed: 23081994]
53. Wardak M, et al. Discriminant analysis of (1)(8)F-fluorothymidine kinetic parameters to predict survival in patients with recurrent high-grade glioma. *Clin Cancer Res*. 2011; 17(20):6553–62. [PubMed: 21868765]
54. Spence AM, et al. NCI-sponsored trial for the evaluation of safety and preliminary efficacy of 3'-deoxy-3'-[18F]fluorothymidine (FLT) as a marker of proliferation in patients with recurrent gliomas: preliminary efficacy studies. *Mol Imaging Biol*. 2009; 11(5):343–55. [PubMed: 19326172]
55. Corroyer-Dulmont A, et al. Detection of glioblastoma response to temozolomide combined with bevacizumab based on muMRI and muPET imaging reveals [18F]-fluoro-L-thymidine as an early and robust predictive marker for treatment efficacy. *Neuro Oncol*. 2013; 15(1):41–56. [PubMed: 23115160]
56. Schwarzenberg J, et al. 3'-deoxy-3'-18F-fluorothymidine PET and MRI for early survival predictions in patients with recurrent malignant glioma treated with bevacizumab. *J Nucl Med*. 2012; 53(1):29–36. [PubMed: 22159180]
57. Enslow MS, et al. Comparison of 18F-fluorodeoxyglucose and 18F-fluorothymidine PET in differentiating radiation necrosis from recurrent glioma. *Clin Nucl Med*. 2012; 37(9):854–61. [PubMed: 22889774]
58. Jain R, et al. Treatment induced necrosis versus recurrent/progressing brain tumor: going beyond the boundaries of conventional morphologic imaging. *J Neurooncol*. 2010; 100(1):17–29. [PubMed: 20179990]
59. van Waarde A, et al. Comparison of sigma-ligands and metabolic PET tracers for differentiating tumor from inflammation. *J Nucl Med*. 2006; 47(1):150–4. [PubMed: 16391199]
60. van Waarde A, et al. Selectivity of 18F-FLT and 18F-FDG for differentiating tumor from inflammation in a rodent model. *J Nucl Med*. 2004; 45(4):695–700. [PubMed: 15073267]
61. Grivennikov SI, Karin M. Inflammation and oncogenesis: a vicious connection. *Curr Opin Genet Dev*. 2010; 20(1):65–71. [PubMed: 20036794]
62. van Waarde A, Elsinga PH. Proliferation markers for the differential diagnosis of tumor and inflammation. *Curr Pharm Des*. 2008; 14(31):3326–339. [PubMed: 19075707]

### Key Points

1. Peptide-based immunotherapy for pediatric brain tumors is associated with the presence of treatment-related heterogeneity including that of pseudoprogression.
2. Conventional MRI has limitations in the assessment of treatment-related heterogeneity, particularly in regards to distinguishing true tumor progression from efficacious treatment responses.
3. Advanced neuroimaging techniques, including diffusion MR, perfusion MR and MR spectroscopy may add value in the assessment of treatment-related heterogeneity
4. Recent delineation of specific response criteria for immunotherapy of adult brain tumors (iRANO) is likely to be relevant to the pediatric population.

## SERIAL MR IMAGING including DIFFUSION PERFORMED

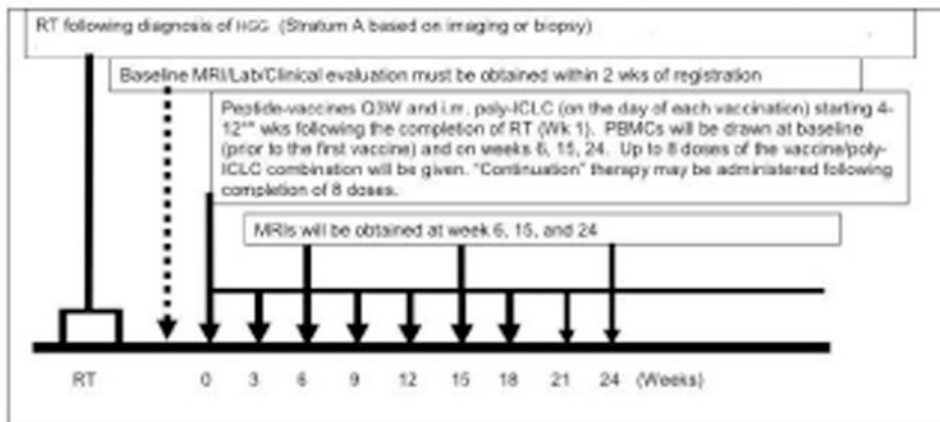


**Figure 1. Example of Timing of MRI scans for New Diagnosis of High-Grade Pediatric Glioma treated with Radiation and Serial Peptide Based Vaccine Therapy**

The time of conventional MRI during the course of peptide-vaccine therapy for this particular strata (A) of the vaccine study was approximately every 6 weeks after initiation of therapy. Strata A of included new diagnosis of high-grade gliomas based on imaging (DIPG) or biopsy and included initial radiotherapy followed by peptide-based vaccine. Note, additional time points of imaging were obtained during clinical pseudoprogression. The timing of serial MRI was different for different strata. Diffusion imaging was integrated with all conventional MRI scans. MRS spectroscopy and perfusion MR were performed in conjunction with only certain conventional MRI scan for logistical reasons.

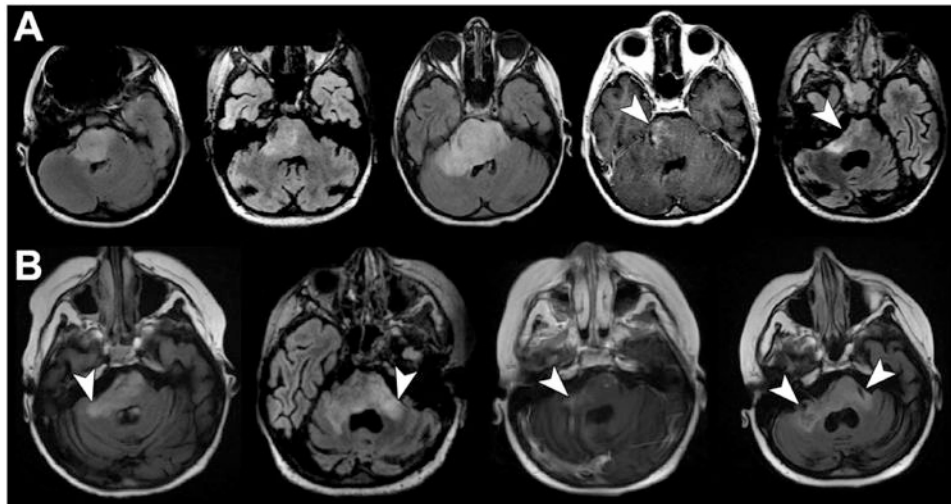


**Figure 2.**  
**A (top) Tumor pseudoprogression.** Left: MR baseline before and after radiation immediately before vaccine therapy. Tumor is unchanged from diagnosis. Middle: after 15 weeks post first vaccine dose, the patient had tumor enlargement (non-enhancing FLAIR hyperintensity) and worsened neurological symptoms. Right: Steroids were started and the MR findings and symptoms improved. **B. (bottom) Development of additional lesions:** Same patient as Figure 2A, but after first pseudoprogression later in the course of the peptide vaccine therapy. Note the development of small lesions (left side of figure) (hyperintense FLAIR signal abnormality in the middle cerebellar peduncle (first in the right middle cerebellar peduncle, and then left middle cerebellar peduncle), that undergo subsequent cystic necrosis and shrinkage on follow up scans (right side of figure).

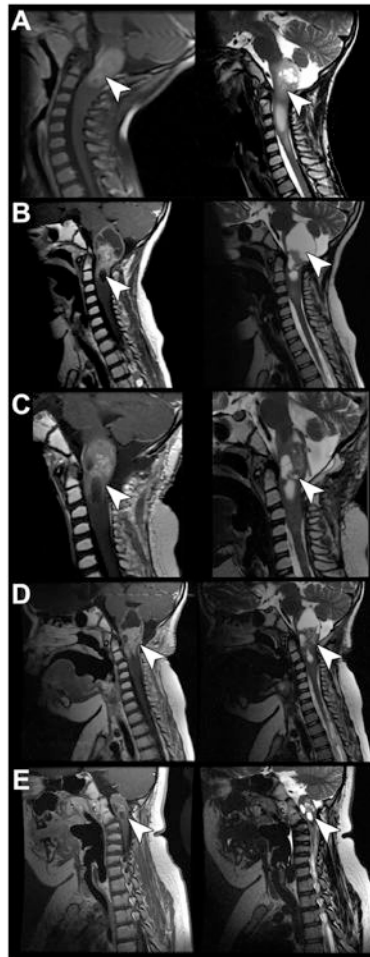


**Figure 3. Biopsy proven pseudoprogression of a cervical medullary anaplastic astrocytoma** 4.5-year-old with a biopsy-proven cervicomedullary anaplastic glioma (top row baseline) who developed worsening neck pain after his 4<sup>th</sup> vaccine, which became increasingly severe immediately after his fifth vaccine, 6.5 months after diagnosis, 4 months after completion of irradiation and 3 months after beginning vaccination. He exhibited neurological worsening and MRI showed formation of a necrotic cyst superior to the tumor in the medullary region (second row). Vaccines were withheld, and the cyst continued to increase in size; his neck pain became debilitating and he underwent laminectomy and cyst decompression 2.5 months later (third row). He had rapid clinical improvement and resolution of the cyst on subsequent MRI scan. Biopsies showed no mitotically active tumor, and he resumed vaccine therapy. Six weeks later, he developed clinical and radiographic worsening with recurrence of neck pain. An MRI showed re-accumulation of the cyst and increased enhancement and size of the solid component, which prompted discontinuation of the vaccine regimen (fourth row). He was started on palliative oral chemotherapy and has shown a dramatic clinical improvement over the next 3 months, is back at school and almost completely off steroids. Five years later the patient is still alive with small stable residual lesion (fifth row)



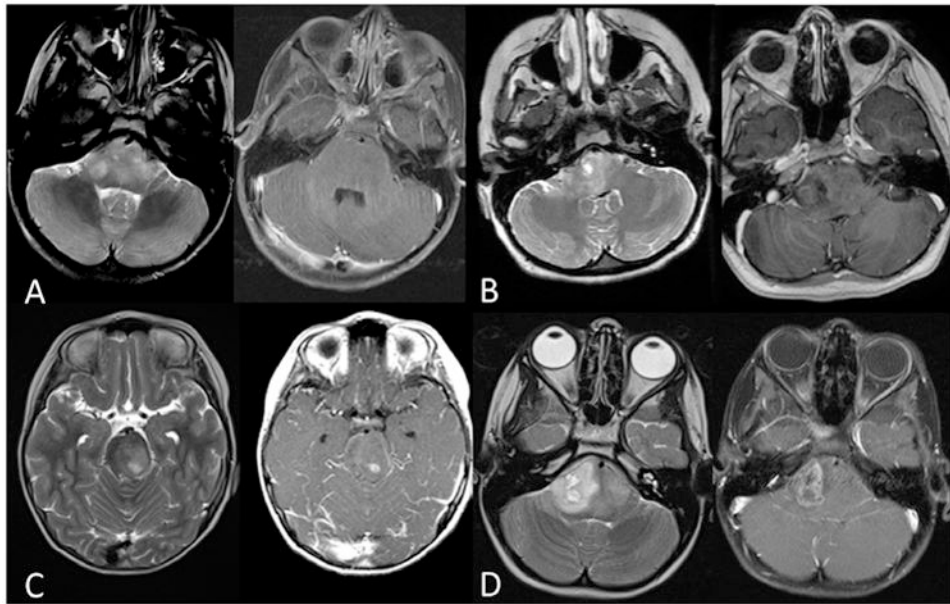


**Figure 4. Focal changes in pediatric DIBG during immunotherapy**

Areas of non cystic changes without enhancement (A), areas of non cystic changes with enhancement (B), areas of cystic changes without enhancement (C), and areas of cystic changes with peripheral enhancement (D).

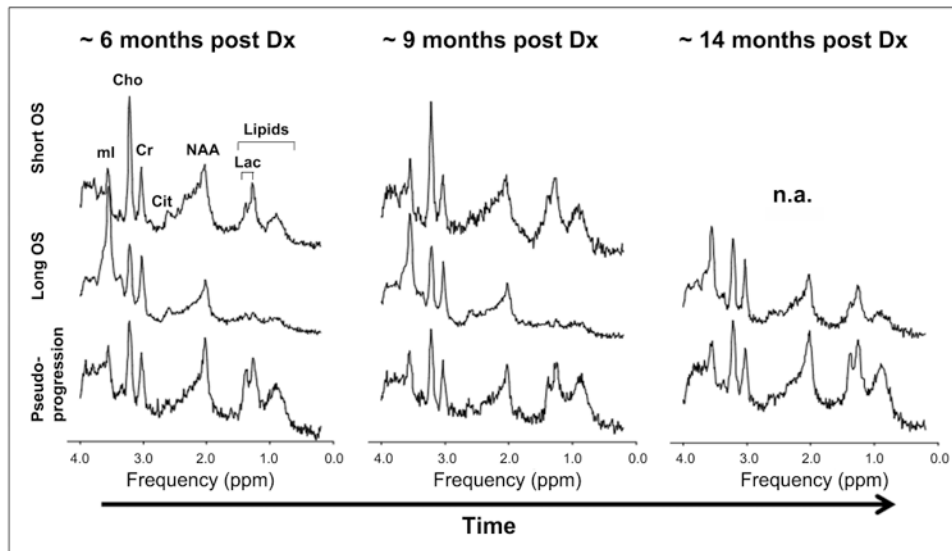


**Figure 5. Comparison of Pseudoproggression case (from Figure 2) with Averaged Spectra of Long Term Survival Group and Short Term Survival Group**

The top row (**Short Term Survival**) shows that there is increase in the choline to creatine ratio between the first two time points. The middle row shows that in the **Long Term Survival Group** there is relative stability in the choline to creatine ratio over time. The bottom row shows the MRS for the **Pseudoproggression** case from Fig. 2 in which there is preservation of choline to creatine ratio across time points. Metabolite levels, including myo-inositol and lipids/lactate remain stable across all three time points in the patient with pseudoproggression (last row).

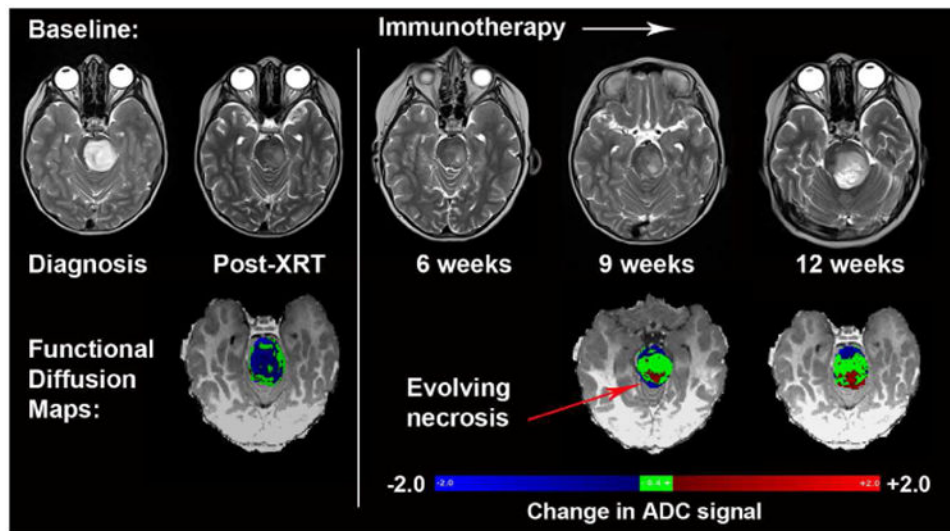


**Figure 6. sfDM to evaluate the spatial-temporal changes in ADC measurements in pediatric DIPG treated with peptide-based vaccination**  
 sfDM demonstrates decrease in ADC signal after radiation (blue voxels, left bottom row). During immunotherapy, focal increase in ADC signal (red voxels, right bottom row) preceded the appearance of necrosis. The stability of the ADC signal (green voxels, right bottom row) is consistent with treatment related necrosis rather than tumor progression.

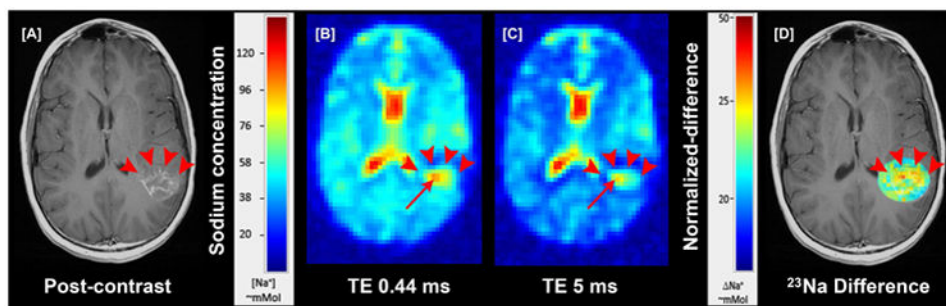


**Figure 7.  $^{23}\text{Na}$ -MR of a necrotic lesion in pediatric subject**

[A] shows a ring enhancing necrotic lesion (red arrowheads); This lesion was a new recurrent lesion, separate from a lesion in the frontal lobe (not shown) that has initially responded to peptide-based vaccine therapy [B] short echo and [C] longer echo  $^{23}\text{Na}$ -MR showing total/extracellular sodium and increased foci in the periphery of lesion (red arrow); [D] co-registered targeted subtracted overlap image show that the periphery of the necrosis (red arrowheads) had increased intracellular sodium (ICS) (red and yellow voxels) and decreased central ICS (bluish and voxels) representing tumor related cavitation/necrosis confirmed to be a **recurrent tumor** by follow up.